Available online at www.sciencedirect.com
ScienceDirect
Optics Communications 271 (2007) 137–141
OPTICS COMMUNICATIONS
www.elsevier.com/locate/optcom

Effect of pulse CO_2 laser annealing on the crystallization of Er^{3+} doped Al_2O_3 thin film to a silica-on-silicon substrate

Qi Song [a,*], Jing-Song Gao [a], Xiao-Yi Wang [a], Tong-Tong Wang [a], Li-Jian Meng [b], Hong Chen [a], Xuan-Ming Zheng [a], Cheng-Ren Li [c], Chang-lie Song [c]

[a] Optical Technology Center, Changchun Institute of Optics, Fine Machine and Physics, CAS, 130033, China
[b] Departamento de Fisica, Instituto Superior de Engenharia do Porto, Rua de São Tomé, 4200 Porto, Portugal
[c] Department of Physics, Dalian University of Technology, Dalian 116024, China

Received 23 March 2006; received in revised form 13 September 2006; accepted 13 September 2006

Abstract

We analyze the effect of the laser annealing on the crystallization of Er^{3+} doped amorphous Al_2O_3 thin films deposited on the silica-on-silicon substrate. These thin films were prepared by the microwave electron cyclotron resonance plasma source and were annealed by pulse CO_2 laser. The Gauss intensity distribution of laser beam was mended at $3\times f$ position in the collimation system. Strong crystallization occurred in Al_2O_3 thin films and liquid phase crystallization was proposed to appear with the increase of laser powers. Photoluminescence intensity enhancement by a factor of 47 around 1.53 μm has been realized by laser annealing process and Raman spectra study has suggested that Er^{3+} emission centers excited by Si nanocrystal (Si-nc) were formed in the Al_2O_3–SiO_2 materials. The dual wavelength energy transfer mechanism between 800 nm and 980 nm is proposed in Er-doped Si-nc in Al_2O_3–SiO_2 thin films.

Keywords: Laser annealing; Alumina thin film; Photoluminescence spectrum

1. Introduction

Because of the very prominent solubility of erbium in the Al_2O_3 matrix, aluminum oxide had been demonstrated to be a more promising and widely investigated material in the erbium doped device applications. However, Er^{3+} ions were often doped onto Al_2O_3 thin films full with amorphous alumina cluster [1]. In order to obtain the more desirable solution and more optical active Er ions in host structure, Al_2O_3 thin films were often annealed for a deep re-crystallization. Recent studies have reported the laser annealing process as a promising approach to modify the microstructure and improve the crystal degree for imparting desirable Al_2O_3 structure [2]. High-power laser materials modification could provide numerous advantages such as a partial ultra-high temperature, controlled thermal penetration, controlled thermal profile, rapid processing and possibility of remote processing and automation [3].

In this work, a study about laser annealing process of Er^{3+} doped Al_2O_3 thin films were presented by using a high-power output CO_2 laser. The liquid-phase transformation was proposed in the laser annealing rather than the thermal annealing. Raman and PL spectrum measurements were carried out to check the formation of Si-nc during this mechanism. Enhanced PL emission by a factor of 47 at 1532 nm indicated that more Er^{3+} emission centers activated by Si nanocrystal (Si-nc) at 800 nm and 980 nm have been formed in this improved Al_2O_3 host crystals. The observation of PL spectrum at 954 nm excitation demonstrated the occurrence of pump mechanism from Si-nc formation to erbium ions.

* Corresponding author. Tel.: +86 04316176077; fax: +86 04315604655.
E-mail address: unlogical0327@yahoo.com.cn (Q. Song).

0030-4018/$ - see front matter © 2006 Elsevier B.V. All rights reserved.
doi:10.1016/j.optcom.2006.09.036

2. Experiment

Al_2O_3 thin films doped with Er ions are deposited on a silica-on-silicon substrate, which is a oxidized silica layer as a buffer layer on a Si substrate. The experimental setup and parameters used in the thin film deposition have been described in our previous work [2]. The thin films were synthesized for 700 nm physics thickness after 3 h deposition, (you mean the thickness of the film is 700 nm?) and the samples were annealed by thermal annealing and laser annealing for comparison. For thermal annealing, the samples are treated in air from 800 °C to 1000 °C, and PL intensity reached the maximum value at 900 °C with an erbium content of 0.45 mol%.

The laser annealing system is shown in Fig. 1. Laser annealing was carried out using a CW carbon dioxide infrared laser operating at 10.6 μm with a 10 ms pulse width, and the diameter of laser beam is 3 mm. A 2 cm-focuse ZnSe concave lens was used to eliminate the Gauss intensity distribution of the CO_2 laser beam. Samples were located at $1\times f$, $2\times f$, and $3\times f$ positions for laser irradiation. The laser was working at an output power of 60 W and irradiation time was controlled by the computer console. In order to keep the constant irradiating power on per area, the irradiation times at $1\times f$, $2\times f$, and $3\times f$ lasted for 800 mS, 1800 mS and 3200 mS.

The PL emissions pumped by a 980 nm semiconductor laser, were monitored through a monochromator by an InGaAs detector and recorded by a lock-in amplifier at room temperature. The PL measurement system is described in our previous paper [2].

Curve a in Fig. 2 shows that the PL intensity distribution in the laser irradiation area at $1\times f$ is decreased from 100% to 61% within 4 cm and is close to the Gauss distribution. Curve b shows that PL intensity distribution at $2\times f$ is equalized within 2 cm and descends from 82% to 73% with the increase of the offset apart from center point. Curve c shows that non-uniform distribution of PL intensity in the laser irradiation area has been well optimized in the extent from 70% to 73% at $3\times f$ position in the collimation system.

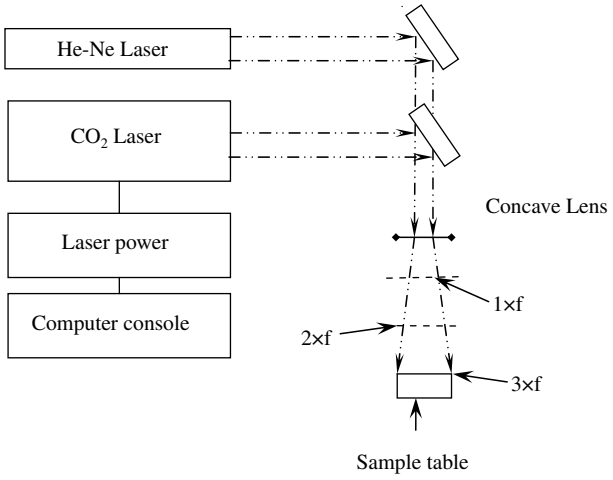

Fig. 1. The schematics of pulse CO_2 laser annealing and collimation system.

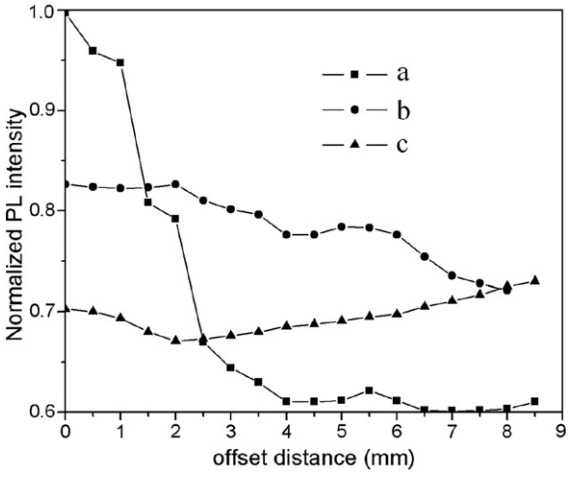

Fig. 2. The Photoluminescence (PL) peak intensity vs the offset from laser irradiation center point. Curves a, b and c represent the PL intensity distribution in the laser irradiation area at $1\times f$, $2\times f$, $3\times f$ location.

Solid points in Fig. 3 shows the dependences of the PL peak intensity with the laser irradiation time under measured irradiation powers of 4.0 J/cm^2 and 1.8 J/cm^2, respectively. Dashed lines represent the dependence of calculated crystallization depth and the laser irradiation time with incidence powers of 4.0 J/cm^2 and 1.8 J/cm^2. Simulated results are obtained from the solid-phase epitaxial model [4]. We deposited the Er-doped Al_2O_3 thin films with an erbium content of 0.45 mol% with the thickness of 312 nm, 452 nm, 608 nm and 698 nm, respectively. After

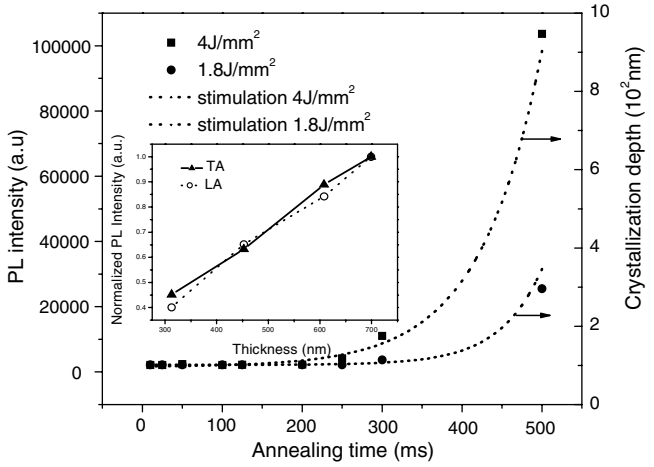

Fig. 3. The dependence of PL intensity and laser irradiation time. The laser powers are 4 J/mm^2 and 1.8 J/mm^2. Dashed lines represent the simulated dependence of the crystallization depth and the laser irradiation time with incidence powers of 4 J/mm^2 and 1.8 J/mm^2, based on the solid-phase epitaxial model. The inset shows that the dependence of PL peak intensity at 1530 nm and the thin film thickness. Solid triangles represent the PL intensity of samples treated by thermal annealing. Circles represent the PL intensity of samples treated by laser annealing.

deposition, samples were annealing at 900 °C for 2 h and 300 mS laser irradiation. The inset in Fig. 3 shows that the PL peak intensity at 1530 nm approximately linearly increases with the increase of thickness of thin film. For comparison, we assume that the PL intensity is proportional to the Al_2O_3 crystallization depth in the simulation during the solid-phase crystallization, which help us compare the crystallization effect both in calculation and experiment. Both results indicate that the time thresholds for the crystallization in experiment and simulation appear degrading with the increase of irradiation power. When it reaches the threshold, the solid phase crystallization process should proceed in the Al_2O_3–SiO_2 layer and more Al_2O_3 and SiO_2 crystals grew instead of amorphous Al_2O_3 and SiO_2 along with the thickness of thin films. When the crystallization depth reaches the total depth of Al_2O_3–SiO_2 layer, the liquid-phase crystallization will take place of the solid-phase crystallization. This crystallization process results in a prominent improvement in PL intensity spectrum, which may be attributed to the fact that Er^{3+}, Al^{3+}, Si^{4+} and O^{2-} ions are reassembled and Er^{3+} emissions center excited by Si-nc are formed in this complicated host. With the increase of irradiation time, The PL intensity reach maximum at 1000 mS and gets 23 times higher than PL intensity at 500 mS, which is not included in the Fig. 3.

Fig. 4a and b shows the surface of both sample A and sample B still keep smooth at a laser power of 4 W/cm^{-2}, with an irradiation of 1000 ms, and 2 h thermal annealing at 900 °C, respectively. The pinholes distributed on the surface as shown in Fig. 4b result from the further increase of the exposure of laser irradiation, which cause the disclosure of Si substrate and a reduction in PL intensity spectrum. Fig. 4d shows that the thin films were peeled off from the substrate because of the intrinsic stress, with the increase of annealing temperature and heat preservation time.

We have measured the Raman shift of the deposited, thermal annealing (TA) and laser annealing (LA) thin films in air. Fig. 5 indicates that the deposited and the 2 h TA at 900 °C, Al_2O_3 thin films are mainly composed of amorphous structure. The peak at 520 cm^{-1} originates from the silicon substrate.

For the LA at 100 ms and 1000 ms, peaks at the 151 cm^{-1} and 480 cm^{-1} for a-Si, 950 cm^{-1} for c-Si, and 300 cm^{-1} for p-Si all appear and increase [5]. The peak position at 942 cm^{-1} is broader and shifted to short-wavelength position compared with 950 cm^{-1} one, which is the typical peak of the SiO_2 system. This shift indicates the combination of Al^{3+} and Si^{4+} in the aluminosilicate structure, because the frequency of the Al–O bond is lower than that of Si–O. Those peaks in Raman spectrum indicates that the liquid-phase transformation drives the Al_2O_3 layer and SiO_2 layer melt into the eutectic Al_2O_3:SiO_2 layer and more Si allotropes appear complex net structure of Al–Si–O. However, 520 cm^{-1} for Si-nc is increased more evidently than other peaks. Because of the better heat conductibility between liquid-phase interface and solid-phase interface, strong crystallization occurs at the boundary between the liquid Al_2O_3:SiO_2 layer and solid Si substrate interfaces. Strong Raman peak at 520 cm^{-1} accounted for (1) the formation of the Si-nc located at the boundary, which results in the significant improvement of PL intensity by exciting more Er^{3+} in Al_2O_3:SiO_2 environment [6]; (2) the development of the Al–Si–O structure in the SiO_2–Al_2O_3 melts, which was normally related to the 3-D network structure in vitreous SiO_2 and Al^{3+} substitution in it [7,8]. Due to the low intensity of erbium, its structure information cannot be obtained by Raman spectra analysis.

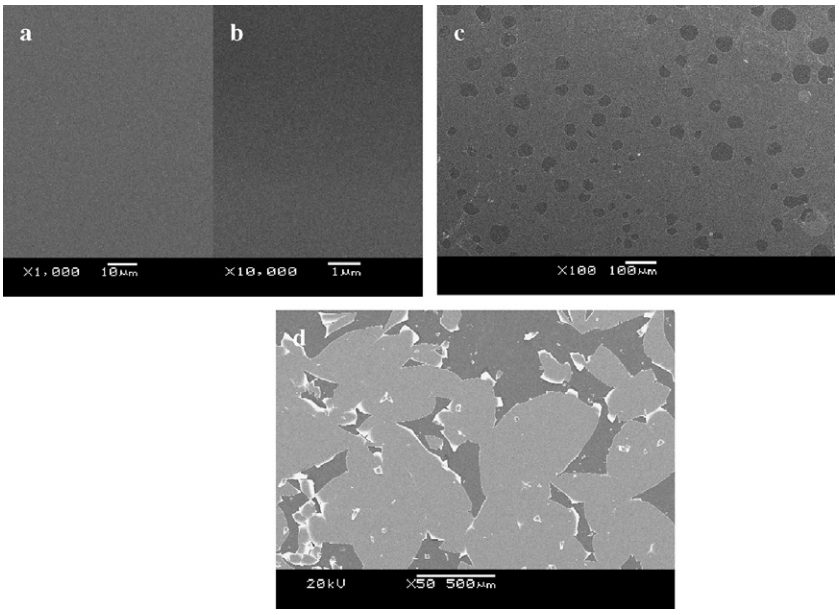

Fig. 4. SEM schematic diagrams of samples treated by laser annealing and thermal annealing. a and b display the surface of sample A annealed at a laser power of 4 W/cm^{-2}, with an irradiation of 1000 ms, and sample B by 2 h thermal annealing at 900 °C.

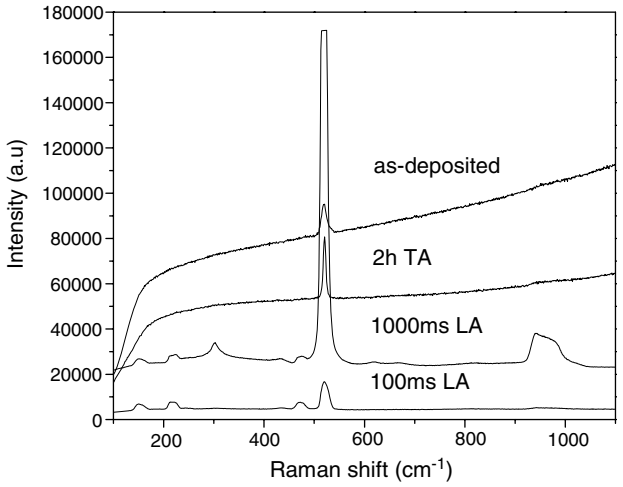

Fig. 5. The Raman spectroscopy of Yb^{3+}: Er^{3+} co-doped Al_2O_3 thin films treated by laser annealing with different irradiation time. As reference the spectra for thermal annealing and deposited films are shown.

Fig. 6 shows PL spectrum corresponding to the $^4I_{13/2} \rightarrow {}^4I_{15/2}$ transition in Er^{3+} ions. PL peak intensity of sample A obtained under a saturated pump power of 4000 mA is as 47 times high as that of sample B pumped with a saturation current value of 1800 mA. There are many reports describing that the presence of Si-nc in Er-doped SiO_2 enhances and expands the effective Er absorption cross-section around 480 nm. However, we chose 980 nm as pump wavelength due to the more efficient absorption and neglectable excitation cross-section of Er ions at this band [9]. In the Al_2O_3–SiO_2 layer, Al_2O_3 can address more Er ions into them due to the similar structure between Al_2O_3 and Er_2O_3. Furthermore, Al_2O_3 and SiO_2 can act as 3-D network host components and Si-nc and Er_2O_3 as lattice defects are induced into host materials [10]. This magnificent improvement of PL intensity indicates that more active Er^{3+} and Si-nc are formed into new emission centers in highly crystallized Al_2O_3–SiO_2 host.

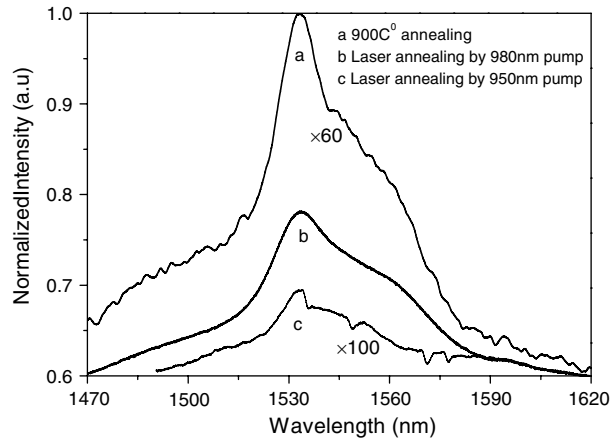

Fig. 6. The PL spectrums of samples of thermal anneal and laser anneal. Sample A treated by laser annealing is pumped by a 954 nm laser and a 980 nm laser with a saturation current value of 4000 mA. Sample B treated by thermal annealing is pumped with a saturation current value of 1800 mA.

The excitation model described in Fig. 7 suggests: When Er-doped Si-nc samples are pumped with a laser beam at 980 nm, photons are absorbed by the Si-nc and electrons are promoted from the valence band E_V to the conduction band E_{C1}. When an Er ion is addressed close to the Si-nc, the energy can be transferred to the Er ion to $^4I_{11/2}$ level. Because Si-nc gives orders of magnitude larger effective excitation cross-section than Er ion at 980 nm, (I did not figure out the meaning of this sentence) the population in $^4I_{11/2}$ increases considerably by the quasi-resonant transfer of energy from Si-nc to Er^{3+}, while cooperative upconversion (CUC) and excite state absorption (ESA) involving $^4I_{11/2}$ level increase with the population in the mean time. At 980 nm pump band, CUC and ESA have become min limitations for PL emission [11]. They both pump Er ions in $^4I_{11/2}$ level to $^4F_{7/2}$ and result in the decrease of the population in $^4I_{11/2}$ level. However, Si-nc could absorb the 490 nm emission of $^4F_{7/2}$ and excite a strong emission at 800 nm. As to this mechanism, theoretical works have described that the electron in E_{C2} is then trapped by a Si = O interfacial state [12]. The recombination of the electron in the interfacial state with a hole in the E_V gives the typical Si-nc light emission at 800 nm [13]. Since the 800 nm Si-nc emission couples well with the $^4I_{9/2}$ level of the Er, the energy can be transferred to the Er ion in it. Therefore, the strong CUC and ESA at 490 nm could be reduced by Si-nc absorption and transferred to another pump wavelength of Er ions. From $^4I_{9/2}$ level a rapid relaxation occurs to the $^4I_{11/2}$ level with the emission of 980 nm photons or with a relaxation to the $^4I_{13/2}$ level and emission of photons at 1530 nm. The Si-nc can absorb a broad wavelength extend under 1000 nm, and Er ions are pumped by 800 nm and 980 nm wavelengths in the energy transfer interaction with Si-nc. In order to demonstrate the energy transfer from Si-nc to Er ions around 980 nm, we excite the sample A with an array laser diode at 954 nm, where Er was proposed to have no absorption. Under the 954 nm excitation, excitation photons were only absorbed by Si-nc and transferred to Er level $^4I_{11/2}$, instead of absorbing by Si-nc and Er ions. Curve c shows the PL

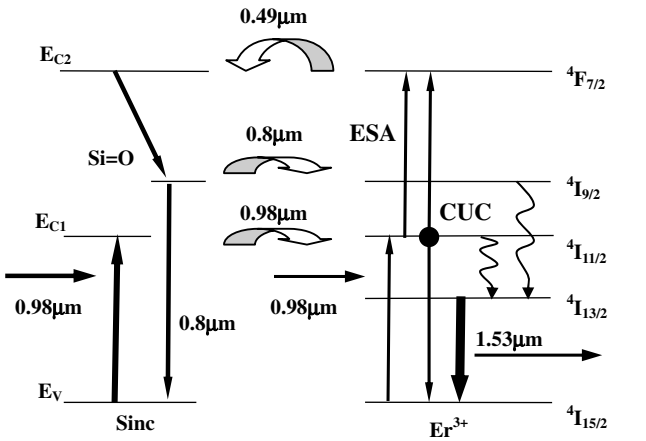

Fig. 7. Energy transfer diagram for Si-nc and erbium interaction system pumped at 980 nm.

emission spectrum of Er ions at 1530 nm pumped by 954 nm. The fractional PL peak split may result from the non-radiation heat effect led by the strong absorption of Si-nc at 954 nm. Thus it can be seen that the PL intensity at 1530 nm emission wavelength could be heavily enhanced by this energy transfer mechanism; i.e. the pump power could be more efficiently transformed by the broad and strong absorption spectrum of Si-nc at 800 nm and 980 nm pump wavelengths.

3. Conclusion

In conclusion, Er^{3+} doped Al_2O_3 thin films were deposited on silica-on-silicon substrate by MW-ECR enhanced RF sputtering and annealed by the pulsed CO_2 laser irradiation. The strong crystallization occurred in Al_2O_3–SiO_2 thin film, and the Gauss intensity distribution of laser beam was mended in the collimation system. In this process, the liquid-state crystallization replaces solid-state process with the increase of the laser power and irradiation time. The Er^{3+} emission centers excited by Si-nc structure are proposed in this Al_2O_3–SiO_2 material and provide us a distinct improvement of PL intensity at 1.53 μm by the dual wavelength energy transfer mechanism at 800 nm and 980 nm in Si-nc. The Si-nc formation and the existence of pump mechanism were demonstrated by Raman spectroscopy and 954 nm excitation.

Acknowledgements

The authors thank Bingbing Sun for stimulating discussion. This work has been supported by the NSFC (Grant No. 60478035 and 69889701).

References

[1] M. Jimenez de Castro, R. Serna, J.A. Chaos, C.N. Afonso, E.R. Hodgson, Nucl. Instrum. Meth. B 166–167 (2000).
[2] Qi Song, Cheng-Ren Li, Jian-Yong Li, Wan-Yu Ding, Opt. Mater. available online since Sep. 2005.
[3] M.J.V. Bell, L.A.O. Nunes, A.R. Zanattaa, J. Appl. Phys. 86 (1999) 11.
[4] Fu Ren Wu, Chen Chao, M.I. Markevich, Chinese J. Luminescence 21 (4) (2000).
[5] O. Ebil, R. Aparicio, S. Heedus, R. Birkmire, NCPV and Solar Program Review Meeting, 2003.
[6] W. Yu, J. He, Y.T. S, H.F. Zhu, Acta Phys. Sinica 53 (2004) 6.
[7] Yasushi Sasaki, Kuniyoshi Ishii, ISIJ Int. 44 (1) (2004) 43.
[8] George Turrell, Jacques Comet, Raman Microscopy Developments and Applications, Academic Press, 1996, p. 39.
[9] A. Shooshtari, T. Touam, et al., Opt. Quant. Electron. 30 (1998) 249.
[10] K. Masaki*, H. Isshiki, T. Kawaguchi, T. Kimura, Opt. Mater. available online 2005.
[11] M. Federighi, F. Di Pasquale, IEEE Photon. Technol. L 7 (3) (1995) 303.
[12] M.V. Wolkin, J. Jorne, P.M. Fauchet, G. Allan, C. Delerue, Phys. Rev. Lett. 82 (1999) 197.
[13] Fabio Iacona, Giorgia Franzò, Corrado Spinella, J. Appl. Phys. 87 (2000) 1295.